5. Innovative Control Paradigms for DC Motors Control

Wilson Pavón PhD. is a Professor of Mechatronic, Architecture Bachelor, and Automation and Control Postgraduate in the Universidad Politécnica Salesiana (Ecuador)
Email: wpavon@ups.edu.ec
https://orcid.org/0000-0002-9319-8815
DOI: 10.00000000

5.1 Introduction

This research proposes innovative control paradigms for DC motors control, integrating variable coefficient fractional-order proportional-integral-derivative (PID), model predictive control (MPC), and State Feedback with Ackerman and Bessel Polynomial Strategies for Optimal Performance. The fractional order is utilized to enhance the control performance of the system. The optimal tuning of the proposed controller is achieved through a hybrid optimization algorithm that combines the particle swarm optimization (PSO) and the genetic algorithm (GA). The PSO algorithm searches for the optimal set of proportional, integral, and derivative gains, while the GA is employed to optimize the fractional order and the controller coefficients. The hybrid algorithm can efficiently obtain the optimal controller parameters and fractional order with a small number of iterations. The proposed variable coefficient fractional order PID controller can be applied to several benchmark control problems, including the inverted pendulum, magnetic levitation system, and water level control. The simulation results show that the proposed controller outperforms the conventional PID controller and the fixed coefficient fractional order PID controller regarding tracking accuracy, disturbance rejection, and robustness. The proposed controller also exhibits good robustness against parameter variations and external disturbances. This research paper proposes a novel variable coefficient fractional order PID controller design with optimal tuning. The article studies the structure of variable-order fractional proportional-integral-derivative (VFPID) controllers for linear dynamical systems. The proposed VFPID controller is designed to regulate the joint variables of a mobile manipulator. The significant contribution of the paper is to fill this gap by presenting a novel approach. To justify the claimed efficiency of the proposed VFPID controller, an improved VFPID controller is also offered in this paper, building the nonlinear relation between the integral gain Ki and derivative gain Kd. The proposed neural network (NNFPID) controller's parameters consist of derivative, integral, and proportional gains in addition to fractional integral and fractional derivative orders. The chapter is

organized as follows, section 5.2 describes the related work, section 5.3 has the methodology, section 5.4 is the results and analysis, and Section 5.5 has the conclusions.

5.2 Related Works

Figure 5.1 illustrates the key authors who have published notable works on fractional PID applied to electrical problems, as observed during the literature review revision.

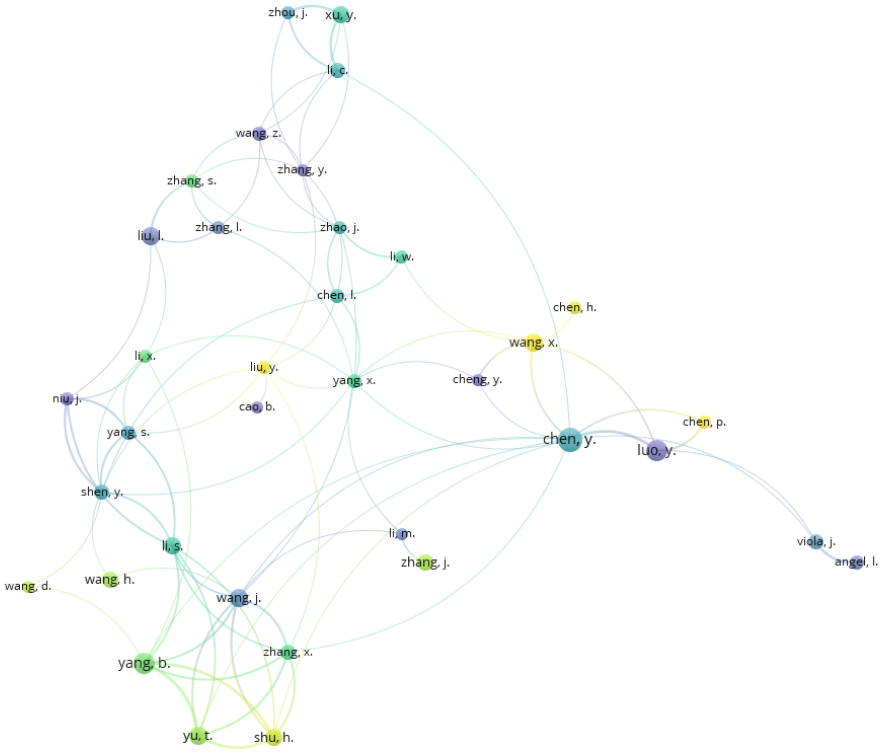

Figure 5.1: Bibliometric revision. Main authors that have published for fractional PID

The article [1] aims to address the advantages of fractional-order PID (FOPID) controllers over conventional integer-order (IO) PID controllers in terms of complexity and implementation. It reviews recent literature, provides analysis, and offers recommendations to understand the benefits of using FOPID controllers despite approximation challenges. Podlubny demonstrated that fractional order PID performs better than integer order PID controllers for fractional order dynamic control systems [2]. Therefore, this research aims to improve the performance of mobile manipulators by proposing a new formulation of fractional order proportional integral (PI)/proportional integral derivative (PID) controller [3], [4]. This research presents an optimal fuzzy proportional-integral-derivative control for a two-wheeled self-balancing robot [5]. The paper of [6] deals with using the graphical tool of the diagrams of Bode, which is used to visualize the required actions so that the proposed systems are stable by including various controllers like PI or PID. The research [7]proposes an optimized Maximum Power Point Tracking (MPPT) controller based on the Grey Wolf Optimization algorithm for Solar photovoltaic systems. The proposed controller is compared to traditional Perturb, Observe, Incremental Conductance, and four metaheuristic algorithms. The models are analyzed for constant and variable irradiations, temperatures, and loads. The comparative results show that the MPPT controller optimized by the Grey Wolf Optimizer algorithm has superior performance, giving an average 6% output power higher than the other controllers under the test scenarios evaluated. The

efficiency of the proposed model was, on average, 3% higher than the Incremental Conductance and Perturb & Observe controllers.

The paper [8] reviews scenario analysis methods to address uncertainty in modern power systems due to renewable energy sources and load variations. It covers scenario generation methods, scenario reduction methods, and scenario quality evaluation indices. The paper discusses new trends in scenario analysis methods and suggests potential research directions for scenario analysis of 100% renewable integrated power systems and integrated multiple energy systems.

The article [9] presents an experimental validation of fractional-order PID (FOPID) controllers on a two coupled tanks system. The paper [10] proposes a charging guiding strategy for electric vehicles (EVs) based on third-generation prospect theory (PT3) and a real-time coupling relationship model. The proposed method analyzes uncoordinated issues and balances the coupling system by guiding EVs based on a dynamic reference point and a full-state prospect description model. An algorithm based on a multi-time scale is used for real-time traffic distribution network simulation. The proposed method can coordinate the distribution of the charging load and relieve traffic pressure. The paper [11] presents a state feedback controller design for open-loop unstable systems using the sand cat swarm optimization (SCSO) algorithm. The SCSO algorithm is a newly proposed metaheuristic algorithm that can efficiently find optimal solutions for optimization problems. The proposed SCSO-based state feedback controller optimizes control parameters with efficient convergence curve speed for three nonlinear control systems: an Inverted pendulum, a Furuta pendulum, and an Acrobat robot arm. Simulation results show that the proposed control method outperforms or has competitive effects compared to well-known metaheuristic-based algorithms. This research [12] proposes an adaptive cooperative co-evolutionary differential evolution method, QGDECC, to schedule railway train delays effectively. The QGDECC utilizes the quantum variable decomposition strategy and increment mutation method to improve convergence speed and strengthen the algorithm's robustness. The proposed method is applied to railway train delay scheduling to eliminate the impact of train delays on the network and minimize the gap between the rescheduled and original train schedules. The experimental results on benchmark functions and actual train operation data show that QGDECC has higher adaptability, faster convergence speed, and accuracy. The paper [13] proposes using the Twin Delay Deep Deterministic (TD3) policy gradient method to optimize the classical Proportional Integral (PI) controller for DC motor speed control using Reinforcement Learning (RL). The TD3 algorithm learns the optimal PI controller dynamics from a simulation environment, incorporating a reward mechanism that minimizes the optimal control objective function. The performance of the RL-based PI controller is compared with integer and fractional order PI controllers tuned by popular metaheuristic optimization algorithms. The results show that the proposed RL-PI method improves control performance, demonstrating the benefits of RL in industrial control applications.

5.3 Methodology

The following practical problem is considered about the speed control of a DC motor. The equation expresses the transfer function relating the output speed to the input voltage.

$$\frac{\dot{\theta}}{V} = \frac{K}{(Js+b)(Ls+R)+K^2}$$

Where:

- J Motor inertia
- b Damping frequency of the mechanical system
- K Constant of electromotive force
- R Electrical resistance
- L Electrical inductance

The parameters below are well known; $J = 0.5, b = 0.01$ y $K = 0.5$.

A DC motor is subjected to a unit step input voltage (1V). Figure 5.2 shows the speed response to the step set.

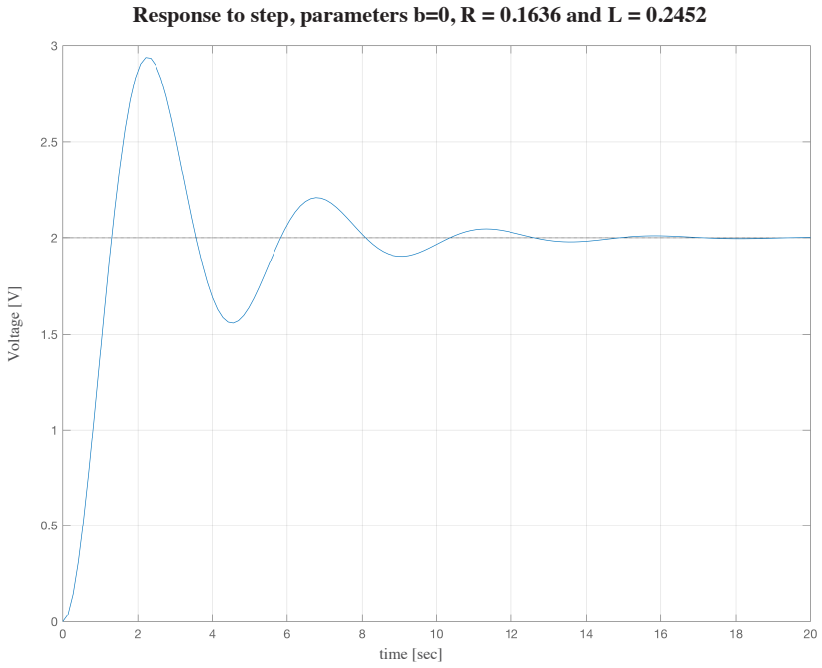

Figure 5.2: DC motor speed response to 1 V step input

Given these parameters, identify the model of the system and, thus, calculate the inductance and resistance of the DC motor. Tip: you have to fix equation 1 to a similar form of the general second-order equation. What is the possibility of simplifying the model assuming b=0? Try to compare it with the initial model. What impact does it have on calculating the value of R and L?

Based on the model obtained, the student must implement a PID controller as a second part of the problem. The controller parameters must be tuned by any method. It is required that the system response reaches a steady state as soon as possible without an overshoot greater than 10 %.

As the third part of the problem, based on the model obtained, the student should propose a state feedback controller to control the motor speed. This controller can be tuned with any method available in the literature. It is required that the system response reaches the steady state as soon as possible without an overshoot more significant than 10%.

Finally, the student must propose a control technique different from those previously offered. Similarly, the same design conditions should be imposed.

Submit a report and present the simulation of the identification and control in SIMULINK/-MATLAB.

5.3.1 First part: System Identification

The equation is:

$$G_1(s) = \frac{K_1}{(Js+b)(Ls+R)+K_1^2} \tag{5.1}$$

and the equation of a second-order system:

$$G_2(s) = \frac{K_2\omega^2}{s^2+2\zeta\omega s+\omega^2} \tag{5.2}$$

Developing equation (5.1) we have:

$$G_1(s) = \frac{K_1}{JLs^2 + (JR + bL)s + (bR + K_1^2)} \tag{5.3}$$

$$G_1(s) = \frac{\frac{K_1}{JL}}{s^2 + \frac{(JR+bL)}{JL}s + \frac{(bR+K_1^2)}{JL}} \tag{5.4}$$

Comparing equations (5.2) and (5.4) we have the following equalities:

$$\frac{K_1}{JL} = K_2\omega^2 \tag{5.5}$$

$$\frac{(bR + K_1^2)}{JL} = \omega^2 \tag{5.6}$$

$$\frac{(JR + bL)}{JL} = 2\zeta\omega \tag{5.7}$$

From (5.5) y (5.6) he have:

$$\frac{K_1}{K_2 JL} = \frac{(bR + K_1^2)}{JL} \tag{5.8}$$

Solving the equation R:

$$R = \frac{K_1}{bK_2} - \frac{K_1^2}{b} \tag{5.9}$$

Replacing in (5.9) the given values and calculating $K_2 \approx 1.987$ (value where the system stabilizes, see Figure 5.2), we have $R = 0.1636\Omega$.

Therefore, to obtain the value of the inductance, it is necessary to know the value of ζ, known as the damping coefficient, which is related to the percentage of damping, MP, according to the equation:

$$MP = 100e^{\frac{-\zeta\pi}{\sqrt{1-\zeta^2}}} \tag{5.10}$$

The value of MP is obtained from the plot of the system response to a step signal, as shown in Figure 5.3, which was calculated to be approximately 47%.

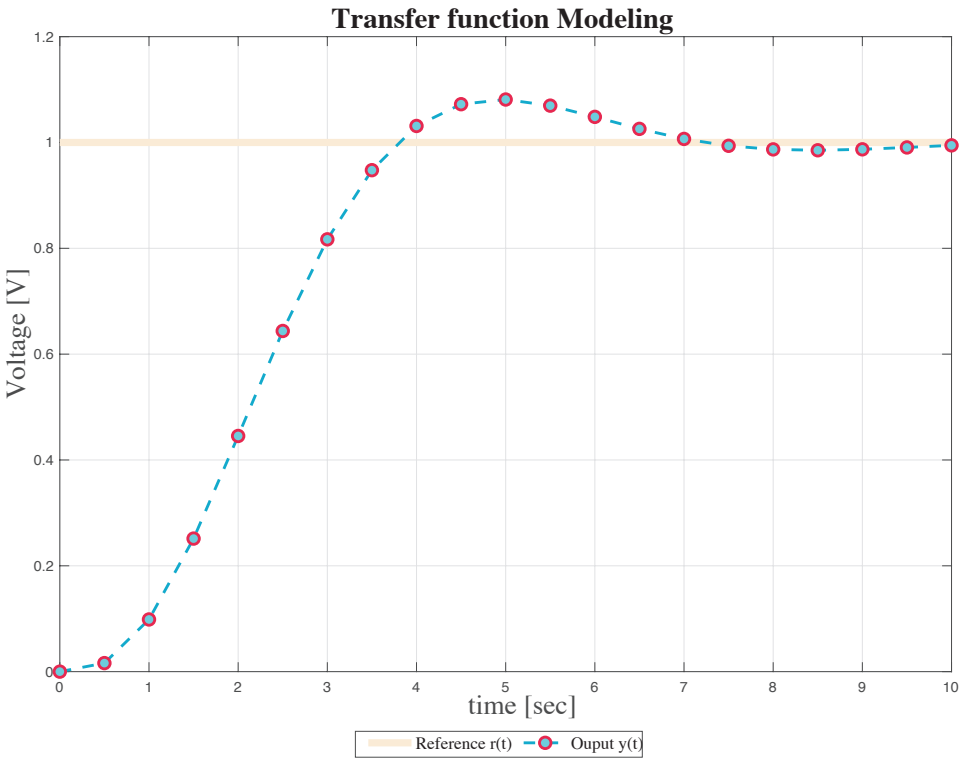

Figure 5.3: System response to a step of 1 V

Solving (5.10) from ζ, it is obtaining $\zeta = 0.2336$.

Then, solving the value of ω de (5.5), $\omega = \sqrt{\frac{K_1}{K_2 JL}}$, and replacing it in (5.7)

$$\frac{(JR + bL)}{JL} = 2\zeta\sqrt{\frac{K_1}{K_2 JL}} \tag{5.11}$$

of the equation (5.11), all values are known except L. Therefore, we will try to solve it for this variable.

Solving (5.11), with the data values of J, K, b and the calculated values of R and ζ, yields the following values of L.

$$L_1 = 0.2592H \qquad L_2 = 258.0144H \tag{5.12}$$

Figure 5.4 shows the system response for the two values of L, with L_1 being the inductance that gives the closest answer to the desired system.

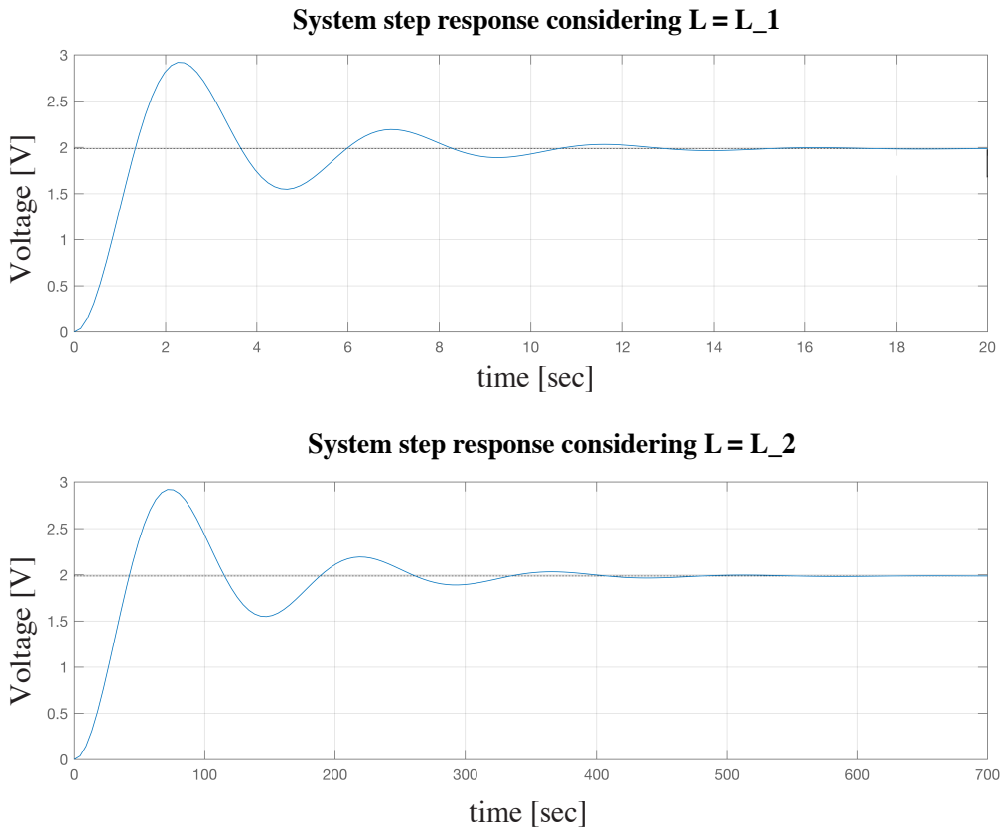

Figure 5.4: Response of the system to the step for the two values of L

Thus, the transfer function of the system is:

$$G(s) = \frac{\dot{\theta}}{V} = \frac{3.58}{s^2 + 0.651s + 1.941} \tag{5.13}$$

5.3.2 System identification with b = 0

Initially in $b = 0$ it is obtained:

$$G_1(s) = \frac{\frac{K_1}{JL}}{s^2 + \frac{R}{L}s + \frac{K_1^2}{JL}} \tag{5.14}$$

Being the equalities:

$$\frac{K_1}{JL} = K_2\omega^2 \tag{5.15}$$

$$\frac{K_1^2}{JL} = \omega^2 \tag{5.16}$$

$$\frac{R}{L} = 2\zeta\omega \tag{5.17}$$

From (5.15) y (5.16) it is obtained:

$$K_2 = \frac{1}{K_1} = 2$$

Now, from (5.16) and (5.17) we have:

$$L = \frac{JR^2}{\zeta^2} \tag{5.18}$$

Thus, we have a parametric equation, L, as a function of R; therefore, it is impossible to directly determine the values of R and L. However, if we take the value of R found in the previous point ($R = 0.16346\Omega$), we have $L = 0.2452H$, and the response of the system is similar to that in Figure 5.4, as shown in 5.5.

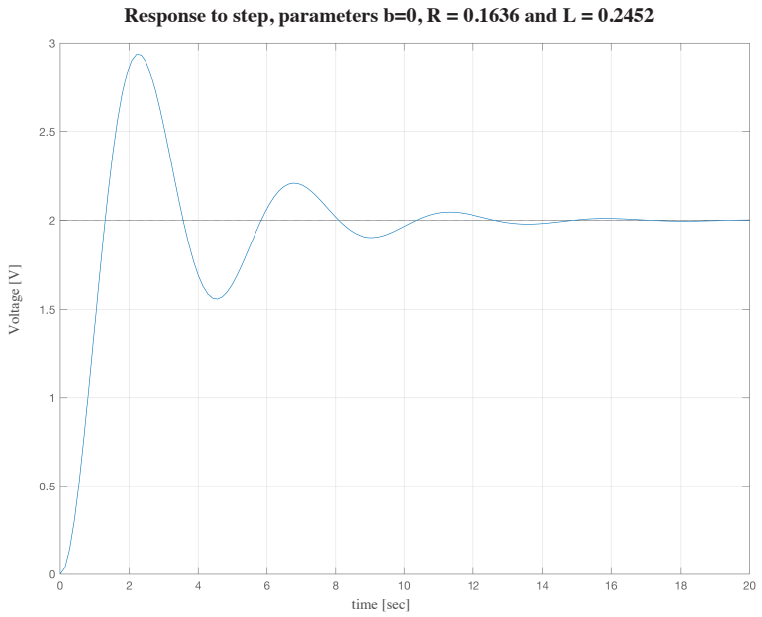

Figure 5.5: Response of the system, with $b = 0$, to the step

Thus, the transfer function of the system is:

$$G(s) = \frac{\dot{\theta}}{V} = \frac{4.078}{s^2 + 0.6671s + 2.039} \tag{5.19}$$

It is then concluded that the value of b does not influence the system too much, which was expected, since some authors ignore it to simplify the modeling of a DC motor.

5.3.3 Part two: PID control

It was decided to develop a PID controller to implement the system in Simulink. Then, to do so, the system was discretized using the command `c2d(TF, T)`, where `TF` is the system's transfer function in continuous time, and T is the sampling period. In this case, $T = 0.05$ seconds was used. Thus the transfer function is:

$$G(z) = \frac{0.004769z + 0.004717}{z^2 - 1.963z + 0.968} \tag{5.20}$$

The system, already with the PID controller, is shown in Figure 5.6.

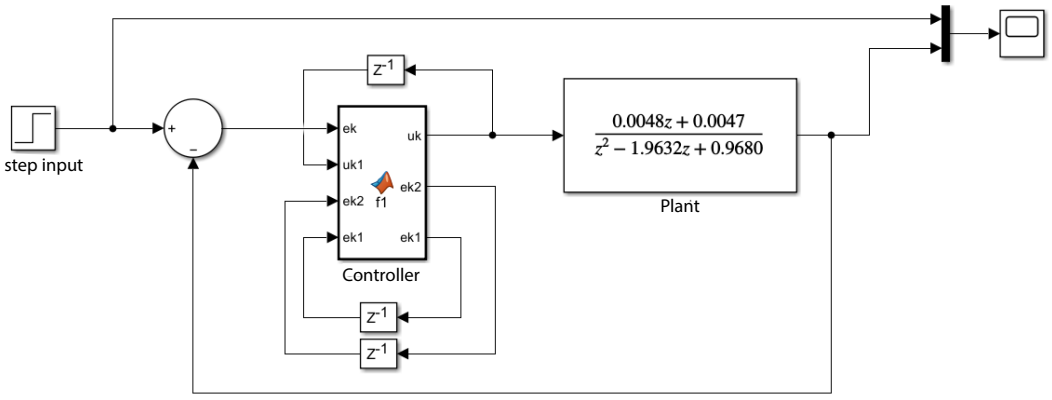

Figure 5.6: System simulation in Simulink

A MATLAB function block is used to program the PID. This block contains the following code.

```
function [uk,ek2,ek1]  = f1(ek,uk1,ek2,ek1)
    kp = 1;
    ki =  4;
    kd =  2;
    T = 0.05;
    uk = uk1 + (kp + ki*T/2 + kd/T)*ek + (-kp + ki*T/2 - 2*kd/T)*ek1 + kd/T*ek2;
    ek2 = ek1;
    ek1 = ek;
end
```

The PID calibration was manual. First, the derivative constant was set to 0 and the integral constant to a minimal value, then the proportional constant was varied until the system reached the reference. The next step was to increase the value of the integrating constant to have a PI control; however, the system became unstable, so giving a discount to the derivative constant was necessary. In this way, the best results were obtained with:

$$K_p = 1; \qquad K_i = 4; \qquad K_d = 2$$

The controller result is shown in Figure 5.7. Whose percentage of overshoot is 0.9743%.

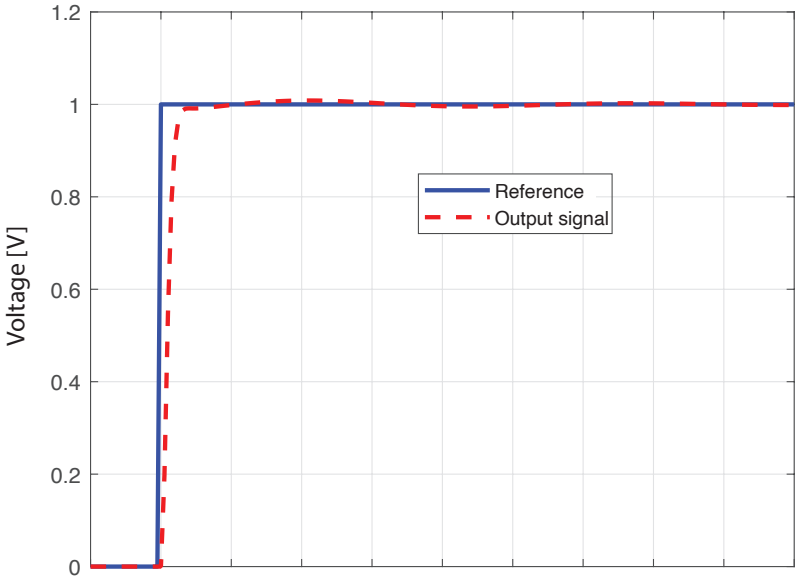

Figure 5.7: System response with PID controller

Figure 5.8 shows the system's response to reference changes. It is clear that the system quickly follows the reference.

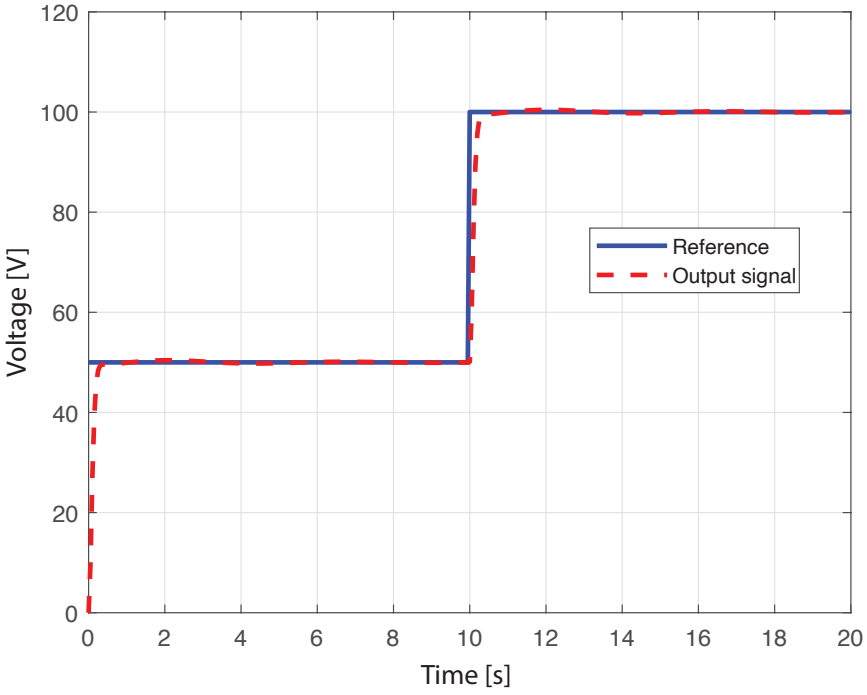

Figure 5.8: Response of the system with PID controller to reference changes

5.3.4 Part three: feedback control

For this part, a control known as an integrating follower was implemented, whose control scheme is shown in Fig. 5.9.

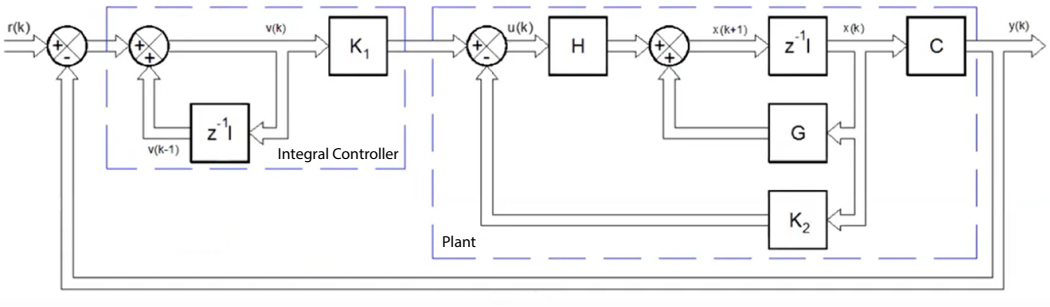

Figure 5.9: Tracking control system with integrator

Being the control law:

$$u(k) = -K_2 x(k) + K_1 v(k) \tag{5.21}$$

This type of controller raises the degree of the system by 1. In this case, the system is of order 2, which will become of order 3 when using the integrating follower.

The controller gains K_1 and K_2 are calculated using Ackerman's formula and Bessel polynomials to bring the poles to a specific location, depending on the desired settling time.

In this case, having seen the response of the PID controller, a settling time of 0.1 seconds is assumed, and the Bessel polynomials of degree 3, taken from Figure 5.1, are used.

Table 5.1: Variables of Roots of Bessel polynomials

Polynomial order	Roots
1	-4.6200
2	$-4.0530 \pm 2.34j$
3	$-5.0093, -3.9669 \pm 3.7845j$
4	$-4.0156 \pm 5.0723j, -5.5281 \pm 1.653j$
5	$-6.4480, -4.1104 \pm 6.3142j, -5.9268 \pm 3.0813j$
6	$-4.2169 \pm 7.53j, -6.2613 \pm 4.4018j, -7.1205 \pm 1.4540j,$
7	$-8.0271, -4.3361 \pm 8.7519j, -6.5714 \pm 5.6786j, -7.6824 \pm 2.8081j$

To obtain the state-space system, the command `tf2ss(num, den)` is used, which returns the state-space matrices of the transfer function, whose numerator and denominator are `num` and `den`, respectively.

The system's response is shown in Figure 5.10, where it is observed how fast the plant follows the reference (settling time of 0.1 seconds); there is an overshoot of 0.6425%.

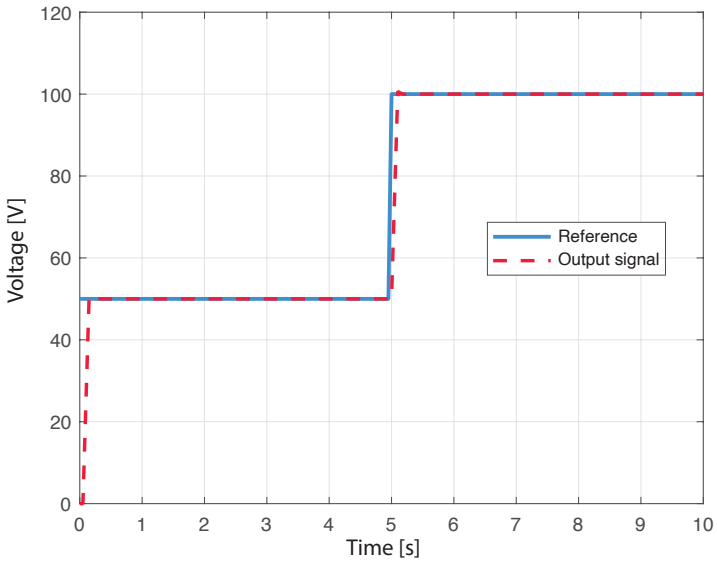

Figure 5.10: System response with integrating follower controller

As a final part, an MPC(Model predictive control) is proposed for the speed control of a DC motor. It is an advanced process control method used by the process industry in chemical plants and oil refineries since the 1980s. In recent years it has also been used in stability models for power systems. MPC can anticipate future events and take control actions accordingly.

This control scheme requires the system in state space to calculate gains that will be used to determine the control variable. The control law for this scheme is:

$$u(k+1) = u(k) + \Delta U(k+1)$$

Being the equations governing the system:

$$Y = Fx(k_i) + \Phi \Delta U$$

$$F = \begin{bmatrix} CA \\ CA^2 \\ \vdots \\ CA^{N_p} \end{bmatrix}$$

$$\Phi = \begin{bmatrix} CB & 0 & 0 & \cdots & 0 \\ CAB & CB & 0 & \cdots & 0 \\ C^2AB & CAB & CB & \cdots & 0 \\ \vdots & \vdots & \vdots & \ddots & \vdots \\ CA^{N_p-1}B & CA^{N_p-2}B & A^{N_p-3}B & \cdots & CA^{N_p-N_c}B \end{bmatrix}$$

After formulating the mathematical model, the next step in designing an MPC control system is calculating the predicted plant output with the future control signal as the

adjustable variable. This prediction is described within an optimization window, with the length of the optimization window being the variable Np (the number of samples).

The future control path is denoted by:

$$\Delta u(k_i), \Delta u(k_i + 1), \ldots, \Delta u(k_i + N_c - 1) \tag{5.22}$$

Where N_c is called the control horizon, which determines the number of parameters used to calculate the future trajectory of the system, there is also the parameter r_w, which is used as a tuning parameter for the controller performance.

5.4 Results and Analysis

The system's response with the MPC controller is shown below, where it is clear that it has a settling time of about 0.3 seconds, and there is no overshoot. Figure 5.11 shows the system's behavior to changes in the reference.

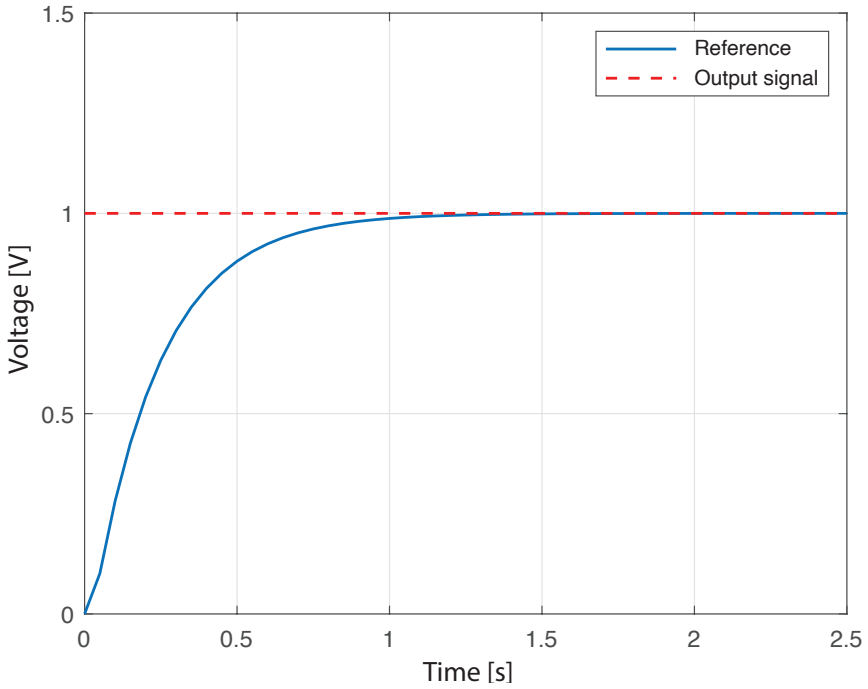

Figure 5.11: System response with MPC controller

It is observed in Figure 5.11 that the system is somewhat slow, almost 1 second in reaching the reference; this is because, although it does not occur here, in Simulink, an over impulse was presented, and if the system with a faster response was made, the over impulse grew to more than 10%.

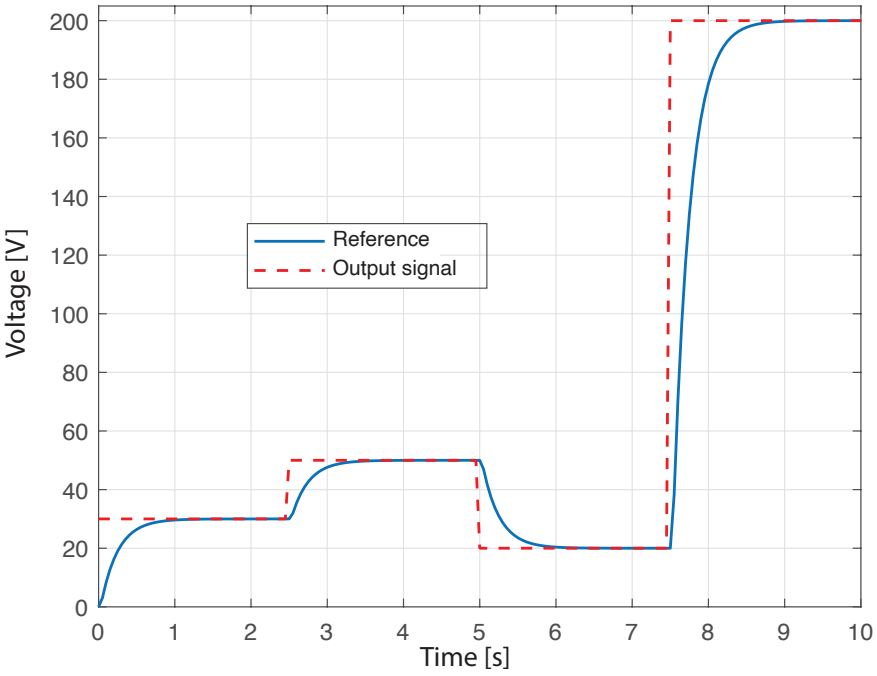

Figure 5.12: Response of the system with MPC controller to reference changes

As said previously, in Figure 5.12, there is no overshoot; when simulating the system in Simulink, there was one, as shown in Figure 5.13. It is approximately 3.6%.

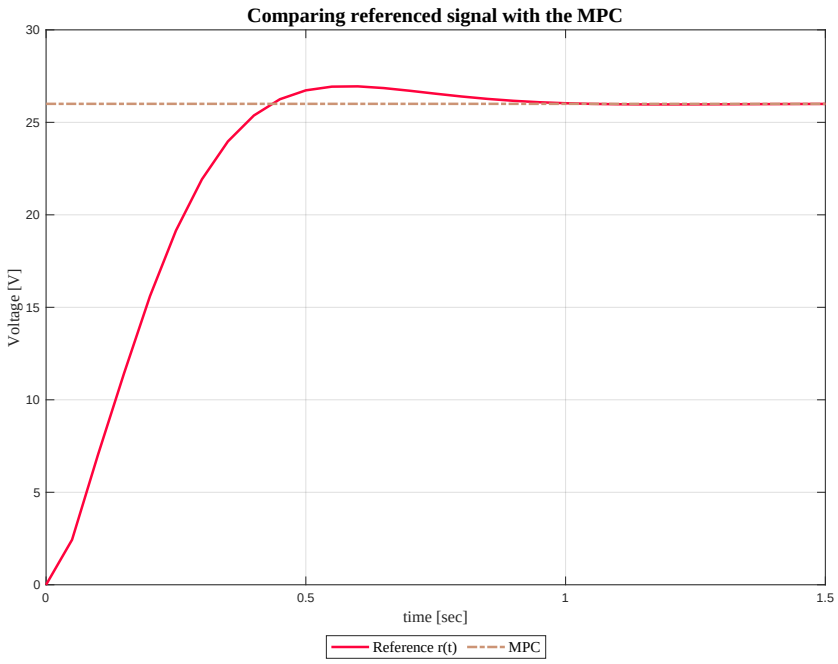

Figure 5.13: System response to a 1V step, in Simulink

The table 5.2 indicates the main results of the controllers. Here it is observed that the integrating follower controller shows the best performance, followed by the PID and finally the MPC.

Table 5.2: Controller results

	PID	**Integrator**	**MPC**
Settling time (s)	0.5	0.1	1
% of the maximum peak	0.9743	0.6425	3.6

Finally, the three controllers are shown in Figure 5.14. It can be seen how the integrator is the first to reach the reference, followed by the PID and then the MPC, with a small pulse sip. The PID shows some oscillation around the reference but quickly stabilizes. In conclusion, all three controllers manage to reach the target.

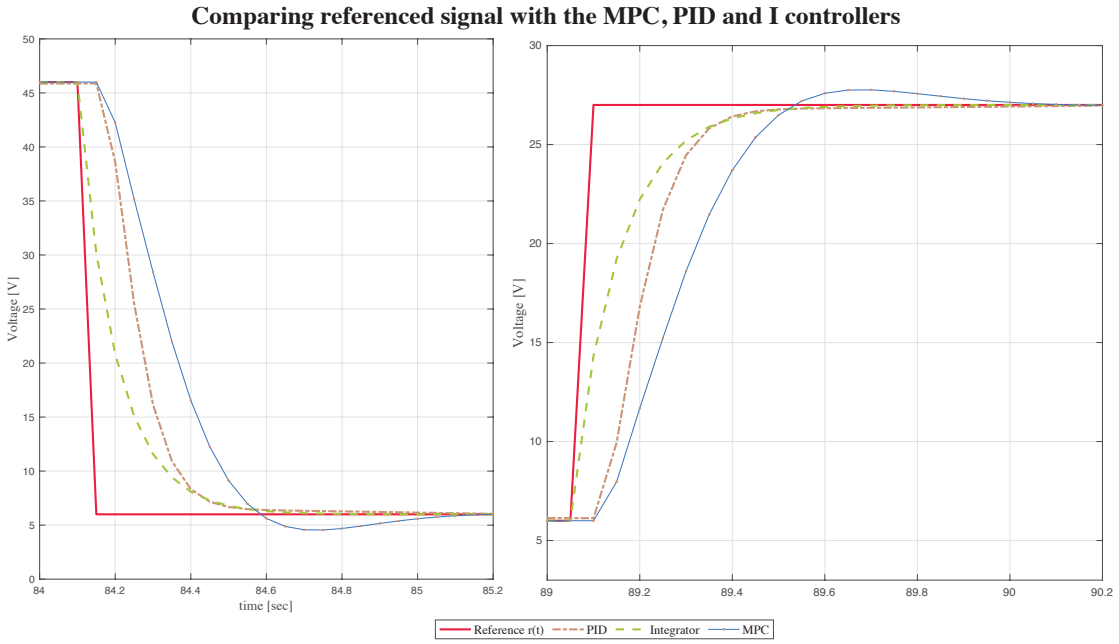

Figure 5.14: Controller response to reference changes

5.5 Conclusions

A practical model for the Direct Current (DC) motor could be developed by utilizing the available data and analyzing the time response graph. This model accurately represents the behavior of the motor and provides valuable insights into its performance. The successful modeling of the DC motor enhances our understanding of its dynamics and facilitates further analysis and optimization in various applications.

Three distinct controllers were developed for the DC motor system through the design process. Each controller exhibited varying performance characteristics, demonstrating suitability for specific application requirements. This achievement highlights the versatility and adaptability of the control system, enabling optimization based on desired outcomes.

The availability of multiple controller options enhances flexibility in addressing diverse operational needs and paves the way for efficient and effective DC motor control in various contexts.

The Model Predictive Controller (MPC) exhibited relatively poorer performance than the other two controllers. However, this does not imply its inefficiency, as further testing is required to ascertain its optimal performance. Therefore, it is recommended to implement the MPC controller on an entire system to evaluate its effectiveness and determine its true potential. This additional experimentation will provide valuable insights and contribute to the ongoing development of efficient control strategies for practical applications.

In summary, fractional order proportional-integral-derivative (FOPID) controllers replace traditional proportional-integral-derivative (PIDs) in real-time control systems. FOPID controllers provide more degrees of freedom than traditional PIDs since their architecture has fractional-order components. This capability, which classical PIDs lack, enables improved controller parameter adjustment, improving closed-loop performance or transient responsiveness when the controllers are applied to nonlinear systems.

Bibliography

[1] A. Tepljakov, B. B. Alagoz, C. Yeroglu, E. Gonzalez, S. H. HosseinNia, and E. Petlenkov, "FOPID Controllers and Their Industrial Applications: A Survey of Recent Results11This study is based upon works from COST Action CA15225, a network supported by COST (European Cooperation in Science and Technology).", *IFAC-PapersOnLine*, vol. 51, no. 4, pp. 25–30, 2018, ISSN: 2405-8963. DOI: https://doi.org/10.1016/j.ifacol.2018.06.014. [Online]. Available: https://www.sciencedirect.com/science/article/pii/S2405896318303045.

[2] I. Podlubny, "Fractional-order systems and PI/sup /spl lambda//D/sup /spl mu//-controllers", *IEEE Transactions on Automatic Control*, vol. 44, no. 1, pp. 208–214, 1999, ISSN: 1558-2523 VO - 44. DOI: 10.1109/9.739144.

[3] A. Fekik, H. Denoun, A. T. Azar, *et al.*, "Adapted Fuzzy Fractional Order proportional-integral controller for DC Motor", in *2020 First International Conference of Smart Systems and Emerging Technologies (SMARTTECH)*, 2020, pp. 1–6, ISBN: 978-1-7281-7407-5. DOI: 10.1109/SMART-TECH49988.2020.00019.

[4] A. Al-Mayyahi, W. Wang, and P. Birch, "Path tracking of autonomous ground vehicle based on fractional order PID controller optimized by PSO", in *2015 IEEE 13th International Symposium on Applied Machine Intelligence and Informatics (SAMI)*, 2015, pp. 109–114, ISBN: 978-1-4799-8221-9. DOI: 10.1109/SAMI.2015.7061857.

[5] R. Sadeghian and M. T. Masoule, "An experimental study on the PID and Fuzzy-PID controllers on a designed two-wheeled self-balancing autonomous robot", in *2016 4th International Conference on Control, Instrumentation, and Automation (ICCIA)*, 2016, pp. 313–318, ISBN: 978-1-4673-8704-0. DOI: 10.1109/ICCIAutom.2016.7483180.

[6] S. Pinzón and W. Pavón, "Diseño de Sistemas de Control Basados en el Análisis del Dominio en Frecuencia", *Revista Técnica "Energía"*, vol. 15, no. 2, pp. 76–82, 2019, ISSN: 1390-5074. DOI: 10.37116/revistaenergia.v15.n2.2019.380.

[7] J. Aguila-Leon, C. Vargas-Salgado, C. Chiñas-Palacios, and D. Díaz-Bello, "Solar photovoltaic Maximum Power Point Tracking controller optimization using Grey Wolf Optimizer: A performance comparison between bio-inspired and traditional algorithms", *Expert Systems with Applications*, vol. 211, no. May 2022, 2023, ISSN: 09574174. DOI: 10.1016/j.eswa.2022.118700.

[8] H. Li, Z. Ren, M. Fan, *et al.*, "A review of scenario analysis methods in planning and operation of modern power systems: Methodologies, applications, and challenges", *Electric Power Systems Research*, vol. 205, no. November 2021, p. 107 722, 2022, ISSN: 03787796. DOI: 10.1016/j.epsr.2021.107722. [Online]. Available: https://doi.org/10.1016/j.epsr.2021.107722.

[9] F. d. J. Sorcia-Vázquez, J. Y. Rumbo-Morales, J. A. Brizuela-Mendoza, *et al.*, *Experimental Validation of Fractional PID Controllers Applied to a Two-Tank System*, 2023. DOI: 10.3390/math11122651.

[10] C. Zhang, K. Peng, L. Guo, C. Xiao, X. Zhang, and Z. Zhao, "An EVs charging guiding strategy for the coupling system of road network and distribution network based on the PT3", *Electric Power Systems Research*, vol. 214, no. PA, p. 108 839, 2023, ISSN: 03787796. DOI: 10.1016/j.epsr.2022.108839. [Online]. Available: https://doi.org/10.1016/j.epsr.2022.108839.

[11] V. T. Aghaei, A. Seyyedabbasi, J. Rasheed, and A. M. Abu-Mahfouz, "Sand Cat Swarm Optimization-Based Feedback Controller Design for Nonlinear Systems", *SSRN Electronic Journal*, vol. 9, no. 3, e13885, 2023, ISSN: 2405-8440. DOI: 10.2139/ssrn.4312627. [Online]. Available: https://doi.org/10.1016/j.heliyon.2023.e13885.

[12] Y. Song, X. Cai, X. Zhou, *et al.*, "Dynamic hybrid mechanism-based differential evolution algorithm and its application", *Expert Systems with Applications*, vol. 213, no. PA, p. 118 834, 2023, ISSN: 09574174. DOI: 10.1016/j.eswa.2022.118834. [Online]. Available: https://doi.org/10.1016/j.eswa.2022.118834.

[13] S. Tufenkci, B. Baykant Alagoz, G. Kavuran, C. Yeroglu, N. Herencsar, and S. Mahata, "A theoretical demonstration for reinforcement learning of PI control dynamics for optimal speed control of DC motors by using Twin Delay Deep Deterministic Policy Gradient Algorithm", *Expert Systems with Applications*, vol. 213, no. PC, p. 119 192, 2023, ISSN: 09574174. DOI: 10.1016/j.eswa.2022.119192. [Online]. Available: https://doi.org/10.1016/j.eswa.2022.119192.